

Quantum Algorithm for Estimating Betti Numbers Using a Cohomology Approach

Nhat A. Nghiem,¹ Xianfeng David Gu,^{2,3} and Tzu-Chieh Wei^{1,4}

¹*Department of Physics and Astronomy, State University of New York at Stony Brook, Stony Brook, NY 11794-3800, USA*

²*Department of Computer Science, State University of New York at Stony Brook, Stony Brook, NY 11794, USA*

³*Department of Applied Mathematics & Statistics,*

State University of New York at Stony Brook, Stony Brook, NY 11794, USA

⁴*C. N. Yang Institute for Theoretical Physics, State University of New York at Stony Brook, Stony Brook, NY 11794-3840, USA*

Topological data analysis has emerged as a powerful tool for analyzing large-scale data. An abstract simplicial complex, in principle, can be built from data points, and by using tools from homology, topological features could be identified. Given a simplex, an important feature is called Betti numbers, which roughly count the number of ‘holes’ in different dimensions. Calculating Betti numbers exactly can be #P-hard, and approximating them can be NP-hard, which rules out the possibility of any generic efficient algorithms and unconditional exponential quantum speedup. Here, we explore the specific setting of a triangulated manifold. In contrast to most known quantum algorithms to estimate Betti numbers, which rely on homology, we exploit the ‘dual’ approach by cohomology, combining the Hodge theory and de Rham cohomology, as well as recent advancement in matrix inversion, multiplication, and block encoding. This cohomology approach requires exponentially fewer qubits than those known homology-based approaches. Our proposed algorithm can calculate its r -th Betti number β_r up to some multiplicative error δ with running time $\mathcal{O}(\log(c_r)c_r/(c_r - \beta_r)\delta)$, where c_r is the number of r -simplex. It thus works best in the regime when the r -th Betti number is considerably smaller than the number of the r -simplices and is exponentially faster than previous known methods.

I. INTRODUCTION

Topology and geometry are lasting and vibrant areas in mathematics. Despite being abstract, topology has laid the groundwork for many important tools that have been widely applied in science and engineering [1–5]. Among them, topological data analysis (TDA) is gaining much attention due to its utility in revealing important topological features of datasets, which, in reality, can be sensitive to noise or sampling errors. Persistent homology, which is built upon algebraic topology, is a powerful method that can probe the topological structure of the underlying dataset. Typically, a collection of high-dimensional data (i.e., vectors) forms an abstract simplicial complex in which the connectivity between data points is controlled by a quantity called length scale.

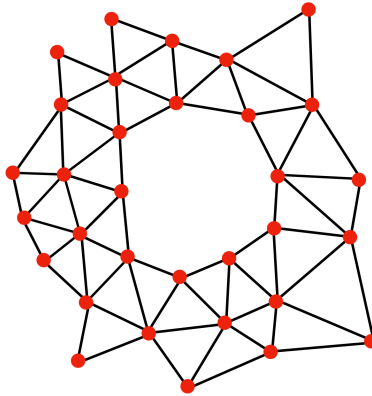


FIG. 1: An (abstract) simplicial complex. Each point (red points), or 0-simplex, might be a vector in a very high dimension.

Given a simplicial complex, one is interested in its Betti numbers, which reveal the number of connected components, loops, holes, etc., of such configuration. The Abelian property and linearity of homology allows the formulation of problems into a linear-algebra framework, which can be more convenient to work with practically. However, the massive dataset volume and its exponential growth in dimensionality induce a very large computational cost, and hence possessing a severe hurdles in practical execution.

Lloyd, Garnerone, and Zanard considered the problem of computing Betti numbers in quantum setting, and their proposed algorithm (the so-called LGZ algorithm) claimed to yield an exponential speedup compared to classical methods [6]. Their underlying approach essentially relies on (simplicial) homology: given a simplicial complex Σ , the k -th Betti number is the rank of the k -th homology group H_k . The rank of such a group (or equivalently, the dimension of such space) is revealed by analyzing the spectrum of the so-called boundary map ∂ , which is a linear map between chain spaces. In Ref. [6], such analysis is then done by applying quantum techniques, such as the quantum phase estimation [7] and sparse matrix simulation [8], leading to the LGZ quantum algorithm. Following Ref. [6], a series of works [9–12] have been substantially improving the running time of the original algorithm [6]. Most recently, a striking result from Ref. [13] clarified some assumptions and performance of the LGZ-like algorithms [6]. In particular, Schmidhuber and Lloyd [13] showed that computing Betti numbers is $\#P$ -hard in the general case and approximating them up to multiplicative error is NP-hard, ruling out the generic efficient estimation of Betti numbers. The potentially exponential advantage of the quantum algorithm can only be obtained if the input is a specified complex instead of a list of vertices (which means that we have to build the complex based on the length scale). Given a specified complex S , the most efficient quantum method (combining [9] and [11]) to estimate the k -th Betti number β_k to some multiplicative error δ is

$$\mathcal{O}\left(\frac{1}{\delta} n \kappa \sqrt{\frac{|c_k|}{\beta_k}}\right),$$

where κ is the conditional number of the so-called Dirac operator [13], n is the number of points (or vertices) in S , and $|c_k|$ is the number of k -simplex at the given length scale. As pointed out in [13], the best classical algorithm can compute the k -th Betti number at a complexity of $\mathcal{O}(|c_k|^3)$. The exponential advantage is recovered in the regime where $\beta_k \rightarrow |c_k|$ and $k \sim \mathcal{O}(n)$. It is reasonable and worthy to question whether the regime $\beta_k \rightarrow |c_k|$ seems to be common in practice, as point clouds usually involve many points with sophisticated connectivity.

In this paper, inspired by the exciting development of recent quantum algorithms for TDA, we attempt to provide a ‘dual’ approach to [6] via cohomology. Another motivation for our method is the discrete Hodge theory, which offers a powerful tool in computational conformal geometry [4]. We focus on the scenario where a simplicial complex S is a uniform triangulation of some closed manifold. By uniform triangulation, we mean that the simplicial complex is built with uniform simplices. For instance, a uniformly triangulated 2-manifold is formed by equilateral triangles or 2-simplices properly gluing together. The same construction holds for arbitrary dimensions, i.e., by gluing higher dimensional objects. According to Schmidhuber and Lloyd [13], this is the case where an exponential speedup is possible, as the description of a simplicial complex is given beforehand instead of a set of vertices and pairwise distances.

As a brief summary, our ‘dual’ approach via cohomology is built upon De Rham cohomology and Hodge theory, as they provide a direct link between the k -th homology/cohomology group and a special group called the harmonic group. Cohomology assigns a real number to each simplex, and therefore, we could store all those numbers in a vector, which again can be stored using a logarithmic number of (qu)bits. Other enabling elements for our algorithm are the recent advances in quantum algorithmic techniques [14–20] that allow handling large matrix operations, such as multiplication, inverting of matrices, and their polynomial transformation. We will see a surprising conclusion that this cohomology framework achieve best performance in the regime $\beta_k \ll |c_k|$, which is opposite to that of LGZ algorithm. It is interesting to mention that many well-known surfaces, such as a sphere, a torus, have low genus numbers which corresponds to low Betti numbers.

This article is organized as follows. First, in section II, we revise some important quantum tools that would contribute as main recipes of our subsequent quantum algorithm. In section III A, we then give some background of de Rham cohomology and Hodge theory in smooth and discrete settings, which contains the key insight into our algorithm. Next, in section III B, we describe the classical procedure for calculating the k -th Betti number in a triangulated manifold. Subsequently, in section IV, we outline the corresponding quantum algorithm for estimating the Betti number. Some analysis and discussion follow subsequently, e.g., in Section VI, including the generalization to different Betti numbers and higher dimensional triangulated manifolds, e.g., in Section V. We conclude in Section VII with some summary and remarks for future exploration.

II. SOME PRELIMINARIES

In this section, we introduce the main quantum ingredients that are needed to construct our subsequent algorithm. We recapitulate the key results for brevity and leave out the details.

First, we define the block encoding.

Definition 1 (Block Encoding Unitary) [18–20] *Let A be some Hermitian matrix of size $N \times N$ whose matrix norm $|A| < 1$. Let a unitary U have the following form:*

$$U = \begin{pmatrix} A & \cdot \\ \cdot & \cdot \end{pmatrix}.$$

Then U is said to be a block encoding of matrix A . Equivalently, we can write:

$$U = |\mathbf{0}\rangle \langle \mathbf{0}| \otimes A + \dots$$

where $|\mathbf{0}\rangle$ denotes the first computational basis state in some larger Hilbert space (of, e.g., multiple qubits). It is quite obvious from the above definition that

$$A_{ij} = (\langle \mathbf{0}| \otimes \langle i|)U(|\mathbf{0}\rangle \otimes |j\rangle), \quad (1)$$

where A_{ij} refers to the entry of A at i -th row and j -th column.

The unitary block encoding of some matrix A as described above allows us to apply the tool of the so-called quantum signal processing [18–20] to achieve arbitrary transformation of A with high efficiency. For instance, as shown in [18, 19], the method yields an optimal algorithm for simulating a Hamiltonian \hat{H} , i.e., implementing the operator $\exp(-i\hat{H}t)$ for arbitrary t given a black box access to entries of \hat{H} . We refer the readers to these original works for details; instead, we delineate the necessary recipe for our subsequent algorithm.

Lemma 1 [18, 20] *Given unitary block encoding of some matrix A of dimension n , then it is possible to construct $\exp(-iAt)$ up to accuracy ϵ in time*

$$\mathcal{O}(d_A(t + \text{poly} \log(1/\epsilon))),$$

where d_A is the required time complexity for preparing the unitary block encoding of A .

Furthermore, the following result for encoding a product of two matrices is useful later and is also proved in Appendix C. Then, we will describe the matrix multiplication and inversion that will be used below.

Lemma 2 (Block Encoding of Product of Two Matrices [20]) *Given a unitary block encoding of two matrices A_1 and A_2 , an efficient procedure exists to construct a unitary block encoding of their product A_1A_2 .*

Lemma 3 (Efficient Matrix Application [17]) *Given a coherent oracle access to some s -sparse, Hermitian matrix \hat{H} of dimension $n \times n$ with eigenvalues' norm bounded in the range $(1/\kappa, 1)$, and a given $n \times 1$ state $|b\rangle$, then there is a unitary U_H that acts in the following way,*

$$U_H |0^m\rangle |b\rangle = |0^m\rangle (\hat{H}/s) |b\rangle + |\Phi_\perp\rangle,$$

where $|\Phi_\perp\rangle$ is some unimportant state (not properly normalized) that is orthogonal to $|0^m\rangle (H/s) |b\rangle$, i.e., $|0^m\rangle \langle 0^m| \otimes \mathbf{1} |\Phi_\perp\rangle = 0$, and $m = \log(n) + 1$. The unitary U_H runs in time

$$\mathcal{O}\left(\log(n), \text{poly}\left(\log\left(\frac{1}{\epsilon}\right)\right)\right),$$

where ϵ is the error tolerance.

Lemma 4 (Matrix Inversion [16]) *Given an oracle access to some s -sparse, Hermitian matrix \hat{H} of dimension $n \times n$ with eigenvalues' norm bounded in the range $(1/\kappa, 1)$, and a given $n \times 1$ state $|b\rangle$. Then, there is a unitary U that acts as follows:*

$$U_H |0^m\rangle |b\rangle = |0^m\rangle (\hat{H}^{-1}/\alpha) |b\rangle + |\Phi_\perp\rangle,$$

where $|\Phi_\perp\rangle$ is some unimportant state (not properly normalized) that is orthogonal to $|0^m\rangle (\hat{H}^{-1}/s) |b\rangle$, i.e., $|0^m\rangle \langle 0^m| \otimes \mathbf{1} |\Phi_\perp\rangle = 0$. The unitary U_H runs in time

$$\mathcal{O}\left(\kappa s \log(n) \text{poly}\left(\log\left(\frac{1}{\epsilon}\right)\right)\right),$$

where ϵ is the error tolerance, and κ is the conditional number of \hat{H} , and α is a (classically computable) constant that guarantees the normalization condition.

We further remark that while in [14], [16] the inverted matrix is assumed to be square and non-singular, some subsequent works, such as [20], were built upon an advanced technique called unitary block encoding (or quantum signal processing [18]), allowing the pseudo inverse if \hat{H} is rectangular and/or has zero eigenvalues. We make an important remark that in Lemma 3 and 4 the eigenvalues' norm is set to be within a fixed range. This can always be achieved by some trivial scaling of a given matrix. Throughout this work, we assume such condition is made. Furthermore, we make an observation that, the factor α appearing in Lemma 4 depends only on the approximation factor that one chooses to approximate, e.g., $1/x$ in [16]. It means that two linear systems in principle can have the same factor α as a result of the quantum linear solver (4).

III. CLASSICAL FRAMEWORK

This section introduces key ingredients from differential geometry that underlie classical and quantum algorithms.

A. de Rham Cohomology and Hodge Theory

De Rham cohomology is a very important tool that encompasses both algebraic and differential topology and can be used to probe the topological structure of smooth manifolds. While in homology, the main objects are spaces (or groups) of chains, in de Rham cohomology, the main objects are spaces of *forms*. The homology group is formed via the equivalence classes of closed chains, whereas in de Rham cohomology, the cohomology group is formed via the equivalence classes of closed forms. Hodge's theory is built on an important observation that each cohomology class has a canonical representative, the so-called harmonic form. A standard result is the Hodge decomposition theorem:

Theorem 1 (Hodge Decomposition) *Suppose M is an n -dimensional closed Riemannian manifold, then*

$$\Omega_k = \text{Img}(d^{k-1}) \oplus \text{Img}(\delta^{k+1}) \oplus H_{\Delta}^k(M), \quad (2)$$

where Ω_k is the space of k -forms, Img denotes the image of a map, d^{k-1} is the exterior derivative map: $\Omega_{k-1}(M) \rightarrow \Omega_k(M)$, δ^{k+1} is the codifferential operator: $\Omega_{k+1} \rightarrow \Omega_k$, and H_{Δ}^k is the space of harmonic k -forms.

In other words, if $\omega \in \Omega_k$, it can be expressed and decomposed as

$$\omega = \delta\Omega + d\eta + h, \quad (3)$$

where $\eta \in \Omega_{k-1}$, $\Omega \in \Omega_{k+1}$, and a special property that it vanishes under the action of d and δ , i.e., $dh = 0$ and $\delta h = 0$. Most importantly, h is unique for each cohomology class, i.e., if ω and ω' lie in the same cohomology class, then they have the same h . Throughout this work, we may abuse the notation by writing δ and d without the superscript.

Generally, de Rham cohomology and Hodge theory work for the smooth setting. But the extension to the discrete setting can be achieved by simply replacing de Rham cohomology with simplicial cohomology by, e.g., identifying k -forms with k -cochains, and so on. The discrete version has been developed and applied extensively in real applications; see, e.g., Refs [3, 4], as d and δ operators can be represented as a linear transformation on a set of corresponding simplices. We use the same notations for both cases, and we treat groups and vector spaces in the same manner, as a vector space is also an Abelian group, and we only work in the Abelian (commutative) setting.

Next, we state two important results that provide a useful insight into our algorithm, to be described below. As mentioned above, each cohomology class has a unique representative, and, therefore, it directly implies the correspondence between the two spaces (or groups), as stated in the two theorems below.

Theorem 2 *Given an n -dimensional closed Riemannian manifold. The k -th de Rham cohomology group is isomorphic to the harmonic k -form group*

$$H_{dR}^k(M) \approx H_{\Delta}^k(M). \quad (4)$$

Another standard and important result that we will employ is the following.

Theorem 3 *The de Rham cohomology group is isomorphic to the simplicial cohomology group*

$$H_{dR}^k(M) \approx H^k(M). \quad (5)$$

We remark that the above two theorems are standard in the areas of differential geometry and algebraic topology, which are explained in standard textbooks, e.g., see [21].

B. Sketch of the Method for Calculating Betti Numbers

Theorems 2 and 3, plus the duality between the simplicial homology and cohomology, show that all these groups are isomorphic, which reveals a potential approach to calculate Betti numbers of a given simplicial complex Σ . Given some k , the k -th Betti number is the rank of the k -th homology group, which is also the rank of the k -th cohomology group. If we regard them as vector spaces, the rank becomes the dimension. We remark that the harmonic forms also form a vector space; therefore, the dimension of such space can be inferred if we know the maximum number of linearly independent vectors. The Hodge decomposition theorem 2 allows us to find the harmonic form given an initial k -form ω , as $h = \omega - d\eta - \delta\Omega$. In fact, the Hodge decomposition theorem works with arbitrary forms, as we will discuss in detail subsequently. The following algorithm 1 summarizes the procedure to find the k -th Betti number.

Algorithm 1 Algorithm for Finding the k -th Betti Number

Input: A set of randomized M k -forms $\{\omega_i\} \in \Omega_k$. A simplicial complex Σ For each $i \in \{M\}$, do:

- 1: 1. Compute the coexact term $\delta\Omega_i$
- 2: 2. Compute the exact term $d\eta_i$
- 3: 3. Find the harmonic form $h_i = \omega_i - d\eta_i - \delta\Omega_i$
- 4: 4. Arrange $\{h_i\}$ as a matrix \mathbb{H} . Find the number \mathcal{K} of linearly independent harmonic forms among all $\{h_i\}$, which is equivalently the rank of \mathbb{H} .

Output: The k -th Betti number is \mathcal{K} .

In the next two sections, we describe how to execute the above procedure in the quantum setting and elaborate on additional details in the Appendix. For convention, throughout the text, we use \vec{x} to denote an arbitrary vector, $|\vec{x}\rangle$ is the quantum state (or normalized vector) corresponding to \vec{x} , and $|\vec{x}|$ denotes its length, i.e., the l_2 -norm. We remark that sometimes we make the following abuse of notation: we typically use $|\mathbf{0}\rangle$ to denote necessary ancillas required to execute algorithms without specifying the actual number of qubits. That being said, if two registers of states being $|\mathbf{0}\rangle$ are provided, they might not have the same dimension. The same convention holds for any $|\textit{Garbage}\rangle$ state since they are irrelevant to our quantum algorithm for computing the rank.

IV. QUANTUM ALGORITHM FOR ESTIMATING BETTI NUMBERS OF TRIANGULATED 2-MANIFOLD

The classical algorithm 1, on which our quantum algorithm is based, can, in principle, be used to find all the Betti numbers. We shall see how its quantum version provides a speedup. To explain our quantum algorithm, we consider specifically the first Betti number for simplicity and illustration. The next section describes how to generalize to higher Betti numbers. The particular simplicial complex that we consider here is the triangulation of a 2-dim manifold, which means that it is composed of many 2-simplices glued together (see Fig. 1). As we will show, the only difference with higher Betti numbers is the specific entries or coefficients of linear equations. We remind readers that our goal now is to construct a quantum version of Algorithm 1. To improve the readability, we will construct each step one by one. We now begin with the computation of the coexact term and then the exact term.

A. Computing Coexact Terms $\delta\Omega$

Let us denote the number of 0-simplices, 1-simplices and 2-simplices as c_0, c_1 , and c_2 , respectively (and hence c_r denote the number of r -simplices). The first step in Algorithm 1 is to compute the coexact term $\delta\Omega$. From equation (3) we have

$$d\omega(f) = d\delta\Omega(f), \quad (6)$$

where f is some 2-simplex. The above yields the following linear equation:

$$A \cdot \vec{\Omega} = B, \quad (7)$$

where A is a sparse matrix $\in R^{c_2 \times c_2}$ which encodes the linear action of $d\delta$, $\vec{\Omega}$ is a column vector containing all $\{\Omega(f_i)\}$, and B encodes the action of $d\omega$. Both $\vec{\Omega}$ and B are $\in R^{c_2 \times 1}$. We want to start from a 1-form vector $\vec{\omega}$ (this is a vector of size $c_1 \times 1$ that contains the values of 1-form ω on all 1-simplices), and then B can be written in a simpler

form as $B = C \cdot \vec{\omega}$, where $C \in R^{c_2 \times c_1}$, which encodes explicitly the operation d with a known expression and is also sparse, and $\vec{\omega} \in R^{c_1 \times 1}$. Therefore, the above equation becomes

$$A \cdot \vec{\Omega} = C \cdot \vec{\omega}. \quad (8)$$

In order to find $\vec{\Omega}$, in principle, we can use the quantum linear solver [14]. However, both A and C are not Hermitian, and do not share the same dimension, and therefore, in order to apply the method, we need to modify the system as follows [14, 22],

$$\begin{bmatrix} \mathbf{0}_{c_2 \times c_2} & A \\ A^T & \mathbf{0}_{c_2 \times c_2} \end{bmatrix} \cdot \begin{bmatrix} \mathbf{0}_{c_2 \times 1} \\ \vec{\Omega} \end{bmatrix} = \begin{bmatrix} \mathbf{0}_{c_2 \times c_2} & C \\ C^T & \mathbf{0}_{c_1 \times c_1} \end{bmatrix} \cdot \begin{bmatrix} \mathbf{0}_{c_2 \times 1} \\ \vec{w} \end{bmatrix}. \quad (9)$$

By doing so we obtain a new matrix that is square and Hermitian. We denote the equation for the new system as

$$A' \cdot \vec{\Omega}' = C' \cdot \vec{\omega}', \quad (10)$$

where $A', C' \in R^{c \times c}$ with $c = c_1 + c_2$, and $\vec{\Omega}'$ contains the solution $\vec{\Omega}$ in its last c_2 entries, and zeros in the remaining. On the right-hand side, $\vec{\omega}'$ contains the 1-form ω in its last c_1 entries. (We note that if one desires the dimensions c_1 and c_2 to be powers of 2, one can always pad 0's in the corresponding matrices and vectors above.) Then the solution has the explicit form:

$$\vec{\Omega}' = A'^{-1} \cdot C' \cdot \vec{\omega}', \quad (11)$$

Given access to entries of A and C (and hence, A' and C'), we can then solve for $\vec{\Omega}'$ using the quantum linear solver [14, 16]. We remark that in this case, aside from inverting a matrix, we also need to apply C' to $\vec{\omega}'$. Such application is in fact a modification of the inverting eigenvalue technique originally introduced in [14] and was also encountered in [22]. More recently, a highly efficient technique for matrix multiplication was outlined in [17], which is built upon the Chebyshev polynomial approach in [16]. Here, we simply integrate the two steps together. We remark that we need to find the coexact term $\delta\Omega$, which can be computed by another round of matrix application, $\delta\vec{\Omega} = R_1 \cdot \vec{\Omega}$, where R_1 is a sparse matrix of size $c_1 \times c_2$ that is the discrete version of δ . In order to apply the same techniques, we made the same modification as above and obtain:

$$\delta\vec{\Omega}' = R'_1 \cdot \vec{\Omega}' \quad (12)$$

$$= R'_1 \cdot A'^{-1} \cdot C' \cdot \vec{\omega}', \quad (13)$$

where R'_1 again is the isometry embedding of R_1 , in a similar form as in Eq. (11). Note that $\delta\vec{\Omega}'$ now contains the coexact values $\delta\vec{\Omega}$ in its first c_1 entries. Since w' is arbitrary, we can safely work with its quantum state $|w'\rangle$ as the length does not matter. Suppose we are equipped with $|w'\rangle$, consecutive application of matrices and matrix inversion (see Eqn 13), which we denote as unitary $U_{\delta\Omega}$, yields the following operation:

$$U_{\delta\Omega} |w'\rangle |\mathbf{0}\rangle = |\psi\rangle = (|\delta\vec{\Omega}'/s_\Omega\rangle \cdot |\mathbf{0}\rangle |\delta\vec{\Omega}'\rangle + |\text{garbage}_1\rangle), \quad (14)$$

where $|\text{garbage}_1\rangle$ is some unimportant state that is orthogonal to $|\delta\vec{\Omega}'\rangle |\mathbf{0}\rangle$; and $s_\Omega = s_{R'_1} s_{C'} \alpha$ which is the product of the sparsity of R'_1 and C' and α , as the application of Lemma 3 contains the sparsity of the matrix, and the usage of Lemma 4 contains the known factor α . We remark that as we will show in appendix A, the sparsity is known. We remind that the notation $|\mathbf{0}\rangle$ is an abbreviation of extra registers that is required in the application of [16, 17].

B. Computing exact term $d\eta$

Now we proceed to the second step in Algorithm 1, which is computing the exact term $d\eta$. This step is very similar to what we had for $\delta\Omega$. From equation (3), we have:

$$\delta\omega(v) = \delta d\eta(v), \quad (15)$$

where v is some 0-simplex. The above yields the following linear equation:

$$K \cdot \vec{\eta} = D \cdot \vec{\omega}, \quad (16)$$

where K is a matrix that encodes the linear action of δd . Proceeding similarly as in the $\delta\Omega$ case, we embed the above system to a square $c \times c$ system (note the dimension) and denote the resultant equation in the enlarged system as

$$d\vec{\eta}' = R'_2 \cdot K'^{-1} \cdot D' \cdot \vec{\omega}', \quad (17)$$

where $d\vec{\eta}'$ contains the exact term $d\eta$ in its first c_1 entries. Application of matrix multiplication and matrix inversion in a similar manner to what we did in the previous part results in a unitary $U_{d\eta}$ that, given $|w'\rangle$, yields the following:

$$U_{d\eta} |w'\rangle |\mathbf{0}\rangle = |\phi\rangle = (|d\vec{\eta}'|/s_\eta) \cdot |\mathbf{0}\rangle |d\vec{\eta}'\rangle + |\text{garbage}_2\rangle. \quad (18)$$

where again, we note that s_η is known.

C. Preparing 1-form state $|w'\rangle$

The above two subsections show that the first step in both is to prepare the 1-form state $|w'\rangle$, which is the state of dimension c that contains the real 1-form w in the last c_1 entries. We note that there are M different initial 1-forms w_j 's, so we need to be able to efficiently prepare many initial states $|w'_j\rangle$'s.

According to the input in Algorithm 1, we note that for any j , entries of $|w'_j\rangle$ are randomly chosen. Therefore, we can pick a short-depth random unitary U_w of dimension $c \times c$. For each index state $|j\rangle$, we have that $U_w |j\rangle$ is the j -th column of U_w , which is also randomized. In order to filter out those top entries, i.e., making these first $c - c_1$ entries to be zero and keeping the last c_1 entries non-zero, we can multiply the vector $U_w |j\rangle$ with a matrix A that is zero everywhere except those last c_1 entries on the diagonal being 1. In other words, we have $A_{ii} = 0$ for $i < c - c_1$ and $A_{ii} = 1$ for any $i \geq c - c_1$. The matrix A is apparently row/column computable, which is equivalent to being coherently accessible. Therefore, we can apply Lemma 3 to obtain $AU_w |j\rangle$, which is our desired 1-form state $|w'_j\rangle$. We have the following result:

Lemma 5 (Preparation of $|w'\rangle$) *Given an input state $|j\rangle$ plus an ancillary register initialized in $|\mathbf{0}\rangle$, then it is highly efficient to construct the unitary U_W that performs the following:*

$$U_W |\mathbf{0}\rangle |j\rangle = |\mathbf{0}\rangle |w'_j\rangle + |\text{Garbage}\rangle, \quad (19)$$

The running time of U_W is

$$\mathcal{O}\left(\log(c), \text{poly}(\log(1/\epsilon))\right),$$

where $|\text{Garbage}\rangle$ is orthogonal to $|\mathbf{0}\rangle |w'_j\rangle$ and ϵ is the error tolerance.

Important Remark: In the following section, for brevity, we make a subtle convention that we focus on the subspace spanned by $|\mathbf{0}\rangle$ in the first register, which means that any further stated operations on $|w'_j\rangle$ (plus possible ancillas) are actually being controlled by $|\mathbf{0}\rangle$ in the Equation 5 of Lemma 5. For convenience, we therefore suppress writing out this register unless necessary.

D. Computing Harmonic Form h

Now we proceed to describe our algorithm to compute h . We first note that while M can be arbitrary large, we choose $M = c_1$ in our algorithm, as it is sufficient for our purpose.

Suppose we begin with $|w'_j\rangle |\mathbf{0}\rangle$, where $|\mathbf{0}\rangle$ is an (additional) ancillary system (we recall the convention regarding the working subspace that we set before). Basically we append extra $|\mathbf{0}\rangle$ to the right of Equation 5 and consider only the subspace spanned by $|\mathbf{0}\rangle$ that appears on the left of $|w'_j\rangle$ in Eqn 5. As we said previously, this can be done by executing any unitary on the first register of $|w'_j\rangle |\mathbf{0}\rangle$, controlled by the second register being $|\mathbf{0}\rangle$ on the left). We then append an extra register initialized as:

$$\frac{1}{2} (|00\rangle - |01\rangle - |10\rangle + |11\rangle),$$

which can be prepared by two Hadamard gates acting on $|1\rangle|1\rangle$. Our whole system is then:

$$\frac{1}{2} \left(|00\rangle - |01\rangle - |10\rangle + |11\rangle \right) |w'_j\rangle |\mathbf{0}\rangle. \quad (20)$$

We note that the quantum 1-form $|w'_j\rangle$ has dimension c , and the actual 1-form w_j is stored in the last c_1 entries, and we need to relocate them to the top c_1 entries so that we can do the subtraction properly (note that $h = w - \delta\Omega - d\eta$). A simple way to achieve this goal is to perform the basis permutation, as we only change the corresponding basis. However, it is unknown (at least to us) whether there is any universal and efficient way to realize arbitrary permutation. Instead, we propose a solution that relies on matrix multiplication. Let A be some symmetric matrix such that $A_{ij} = 1$ if $i \leq c_1, j > c - c_1$ (note that we need to assume $c \geq 2c_1$, but this can always be made possible as we only need to enlarge the system and set the extra coefficients to be zero), and 0 otherwise. Then, a simple multiplication of A with $|w'_j\rangle$ will exactly relocate those last c_1 entries. Since A is easily computable, applying Lemma 3 allows us to implement such quantum multiplication. We have the following lemma:

Lemma 6 *Given a quantum state $|x'\rangle$ of dimension c that is non-zero in the last c_1 rows, and zero otherwise. Let \vec{x} be the vector with the same entries as $|x'\rangle$ but instead have those non-zero entries in the first c_1 rows (with the same order of entries). Then, the following operation can be achieved efficiently:*

$$U_C |x'\rangle |\mathbf{0}\rangle = |\vec{x}|x\rangle |\mathbf{0}\rangle + |\text{Garbage}\rangle, \quad (21)$$

where $|\text{Garbage}\rangle$ is some state that is orthogonal to $|x\rangle|\mathbf{0}\rangle$.

Note that the state $|x'\rangle$ represents a normalized vector, so the sub-vector \vec{x} is guaranteed to have a norm less than unity. Now we specifically look at the part $|00\rangle|w'_j\rangle|\mathbf{0}\rangle$. Using the above Lemma, we can apply U_C , which is controlled by the first two qubits being $|00\rangle$, to the state $|w'_j\rangle$ so as to produce the shifted version of the vector $|w'_j\rangle$, for which we denote simply as $|w_j\rangle$. (Without confusion, we will use the language that U_c is applied to $|w'_j\rangle$ controlled by $|00\rangle$.) To be more specific, the state $|00\rangle|w'_j\rangle$ is transformed to:

$$|\phi_1\rangle = |00\rangle (|\vec{w}_j|w_j\rangle |\mathbf{0}\rangle + |\text{Garbage}\rangle). \quad (22)$$

Next, we consider the part $|01\rangle|w'_j\rangle|\mathbf{0}\rangle$. We aim to apply $U_{\delta\Omega}$ to $|w'_j\rangle|\mathbf{0}\rangle$ being controlled by the first two qubits being $|01\rangle$. We then obtain the following state:

$$|\phi_2\rangle = |01\rangle \left(|\delta\vec{\Omega}'_j|/s_\Omega \cdot |\delta\vec{\Omega}'_j\rangle |\mathbf{0}\rangle + |\text{garbage}\rangle \right). \quad (23)$$

Similarly, we consider the part $|10\rangle|w'_j\rangle|\mathbf{0}\rangle$. We apply $U_{d\eta}$ being controlled by the first two qubits being $|10\rangle$ to obtain:

$$|\phi_3\rangle = |10\rangle \left(|d\vec{\eta}'_j|/s_\eta \cdot |d\vec{\eta}'_j\rangle |\mathbf{0}\rangle + |\text{garbage}\rangle \right). \quad (24)$$

For the last part $|11\rangle|w'_j\rangle|\mathbf{0}\rangle$, we simply flip the first bit in the register $|\mathbf{0}\rangle$ controlled by the register $|11\rangle$. In other words, we transform $|11\rangle|w'_j\rangle|\mathbf{0}\rangle$ into

$$|11\rangle|w'_j\rangle|\tilde{\mathbf{0}}\rangle,$$

where $\tilde{\mathbf{0}}$ denotes one less 0 from $\mathbf{0}$.

So far we have transformed the equation 20 into:

$$|\phi\rangle = \frac{1}{2} \left(|\phi_1\rangle - |\phi_2\rangle - |\phi_3\rangle + |11\rangle|w'_j\rangle|\tilde{\mathbf{0}}\rangle \right). \quad (25)$$

Denote the whole unitary process that transforms the initial state $|\mathbf{0}\rangle|j\rangle$ (which actually began from Lemma 5) to the above state as U_ϕ , specifically, which is $|00\rangle\langle 00| \otimes U_C \otimes I + |01\rangle\langle 01| \otimes U_{d\eta} \otimes I + |10\rangle\langle 10| \otimes U_{d\eta} \otimes I + |11\rangle\langle 11| \otimes I \otimes X_1$. As a summary, by explicitly including the previously suppressed register and all the ancillas, we have:

$$U_\phi |\mathbf{0}\rangle |00\rangle |j\rangle |\mathbf{0}\rangle = |\mathbf{0}\rangle |\phi\rangle + |\text{Garbage}\rangle. \quad (26)$$

The reason why we have $|\phi\rangle$ entangled with $|\mathbf{0}\rangle$ on the r.h.s. is due to the convention that we have made after Lemma 5, as everything was done being (additionally) controlled by $|\mathbf{0}\rangle$ in Eqn. 5.

Now we use a different procedure with the state $|\mathbf{0}\rangle|00\rangle|i\rangle|\mathbf{0}\rangle$. Let s_m be some integer value that is greater than both $s_\Omega + s_\eta$, e.g., $s_m = s_\Omega + s_\eta + 1$. We use controlled rotation gates to transform the register $|00\rangle$ to

$$\frac{1}{s_m} |00\rangle + \frac{s_\Omega}{s_m} |01\rangle + \frac{s_\eta}{s_m} |10\rangle + G |11\rangle,$$

where G in the above state refers to the required normalization factor, i.e.,

$$G = \sqrt{1 - \frac{1}{s_m^2} - \frac{s_\Omega^2}{s_m^2} - \frac{s_\eta^2}{s_m^2}}.$$

We again note that as the linear matrices that implement d and δ are known, their sparsities are also known. The above state can be obtained from $|00\rangle$ by the following procedure. We first use rotation gate to transform $|00\rangle$ to:

$$|0\rangle \left(\sqrt{1/s_m^2 + (s_\eta/s_m)^2} |0\rangle + \sqrt{(s_\Omega/s_m)^2 + G^2} |1\rangle \right).$$

We then perform two controlled rotation gates. The first one is controlled by $|0\rangle$, and the second is controlled by $|1\rangle$ in the second register. More specifically, we transform:

$$\sqrt{1/s_m^2 + (s_\eta/s_m)^2} |00\rangle \rightarrow \sqrt{1/s_m^2 + (s_\eta/s_m)^2} \left(\frac{1/s_m}{\sqrt{1/s_m^2 + (s_\eta/s_m)^2}} |00\rangle + \frac{s_\eta/s_m}{\sqrt{1/s_m^2 + (s_\eta/s_m)^2}} |10\rangle \right), \quad (27)$$

and

$$\sqrt{(s_\Omega/s_m)^2 + G^2} |01\rangle \rightarrow \sqrt{(s_\Omega/s_m)^2 + G^2} \left(\frac{s_\Omega/s_m}{\sqrt{(s_\Omega/s_m)^2 + G^2}} |01\rangle + \frac{G}{\sqrt{(s_\Omega/s_m)^2 + G^2}} |11\rangle \right). \quad (28)$$

We thus obtain our desired two-qubit state and the other part, and we denote for convenience the whole process as U , i.e.,

$$U |\mathbf{0}\rangle |00\rangle |i\rangle |\mathbf{0}\rangle = |\mathbf{0}\rangle \left(\frac{1}{s_m} |00\rangle + \frac{s_\Omega}{s_m} |01\rangle + \frac{s_\eta}{s_m} |10\rangle + G |11\rangle \right) |i\rangle |\mathbf{0}\rangle |\mathbf{0}\rangle \equiv |\Phi\rangle. \quad (29)$$

We then make the following crucial observation:

$$\langle \mathbf{0} | \langle i | U^\dagger U_\phi | \mathbf{0} \rangle | j \rangle = \langle \Phi, \phi \rangle = \frac{1}{s_m} \left(\langle i | (\vec{w}_j - |\delta\vec{\Omega}'_j\rangle \cdot |\delta\vec{\Omega}'_j\rangle - |d\vec{\eta}'_j\rangle \cdot |d\vec{\eta}'_j\rangle) \right), \quad (30)$$

which allows us to compute the components in the above combination of vectors,

$$\vec{w}_j - |\delta\vec{\Omega}'_j\rangle \cdot |\delta\vec{\Omega}'_j\rangle - |d\vec{\eta}'_j\rangle \cdot |d\vec{\eta}'_j\rangle,$$

which is exactly the harmonic form h_j associated with the initial 1-form w_j . Therefore, the inner product $\langle \Phi, \phi \rangle$ is exactly the i -th entry of the j -th harmonic form h_j . By definition, the unitary $U^\dagger U_\phi$ is exactly the unitary block encoding of \mathbb{H} (where \mathbb{H} was defined in algorithm 1), scaled down by a factor s_m . We note that the scaling-down factor does not affect the subsequent algorithm, as the kernel of a scaled-down matrix is the same. In fact, in the Appendix, we will show that s_m is actually not large, of order unity only. Therefore, we omit the factor s_m in subsequent discussion.

Given the unitary encoding of \mathbb{H} , it is trivial to obtain the unitary encoding of \mathbb{H}^\dagger , as it is just a matter of transposition (note that \mathbb{H} is real). Therefore, it is straightforward to apply Lemma 2 to obtain the unitary block encoding of $\mathbb{H}^\dagger \mathbb{H}$. Since all the forms w_j 's (and hence, their harmonic forms) are real, it is safe to use $\mathbb{H}^T \mathbb{H}$ simply. Note we shall use $\mathbb{H}^T \mathbb{H}$ instead of \mathbb{H} because \mathbb{H} is not generally symmetric, while $\mathbb{H}^T \mathbb{H}$ is apparently symmetric. Lemma 1 then allows us to efficiently simulate $\exp(-i\mathbb{H}^T \mathbb{H}t)$. The next goal is to estimate the dimension of $\text{Ker}(\mathbb{H}^T \mathbb{H})$, where Ker refers to the kernel space. This is similar to what was done in Ref. [6], where the authors also employed the simulation of the boundary map combined with quantum phase estimation method [7] to extract the kernel of the corresponding boundary operator, which in turn reveals the Betti numbers. Basically, we first generate the following mixed state:

$$\rho = \frac{1}{c_1} \sum_{j=1}^{c_1} |j\rangle \langle j|,$$

by first preparing $\sum_{j=1}^{c_1} |j\rangle / \sqrt{c_1}$ and using CNOT gates to copy the bitstring to another ancillary system initialized in $|0\rangle$. Tracing out either system yields ρ . We can then run the quantum phase estimation algorithm with the unitary action being $\exp(-i\mathbb{H}^T \mathbb{H}t)$ and the input state being ρ . Note that kernel space corresponds to the eigenvectors with zero eigenvalues; therefore, for those eigenvectors, the quantum phase estimation algorithm will output the zero-bit string on the extra register that holds the outcome of phase estimation. Since the mixture ρ is uniform, the probability of measuring zeros on the extra register in the quantum phase estimation circuit is:

$$p_0 = \frac{\dim \text{Ker}(\mathbb{H}^T \mathbb{H})}{c_1}. \quad (31)$$

Therefore, we can estimate $\dim \text{Ker}(\mathbb{H}^T \mathbb{H})$ by repeating the algorithm to extract the measurement outcomes. We note that the phase estimation step also appeared in [6] and was pointed out in [13] that quantum counting [23] can be used instead to estimate p_0 . In order to estimate p_0 to additive accuracy ϵ , it takes $\mathcal{O}(1/\epsilon)$ time steps by quantum counting. However, $\dim \text{Ker}(\mathbb{H}^T \mathbb{H})$ is an integer, and we require the ability to estimate it to some multiplicative error δ_d . One can choose

$$\epsilon = \delta_d \frac{\dim \text{Ker}(\mathbb{H}^T \mathbb{H})}{c_1}$$

to achieve such a goal. As the last step in our algorithm, the following result shows that $\dim \text{Ker}(\mathbb{H}^T \mathbb{H})$ is exactly $\dim \text{Ker}(\mathbb{H})$.

Lemma 7 *Let $X = A^T A$ be some matrix of size $d \times d$ (A is not necessary to be square). Then $\text{Ker}(X) = \text{Ker}(A)$.*

Proof: (\rightarrow) It is obvious that $\text{Ker}(A) \subset \text{Ker}(X)$, since if $Ax = 0$ (i.e., $x \in \text{Ker}(A)$) then $A^T Ax = 0$. (\leftarrow) Let $x \in \text{Ker}(X)$, hence $A^T Ax = 0$. We consider the inner product

$$x^T A^T Ax = x^T (A^T Ax) = 0.$$

But $x^T A^T = (Ax)^T$, and, therefore, the above equality is equivalent to

$$(Ax)^T Ax = 0.$$

The above product is also the definition of a norm of a real vector Ax , which is, by definition, equal to 0 if and only if $Ax = 0$. It implies that $x \in \text{Ker}(A)$. Our proof is thus completed.

The result sheds some light on how the Betti numbers can be calculated. We remark that $\dim \text{Ker}(\mathbb{H})$ is not the Betti number itself but the rank of \mathbb{H} which is $c_1 - \dim \text{Ker}(\mathbb{H})$ is equal to β_1 – the first Betti number. Therefore, the ability to find $\dim \text{Ker}(\mathbb{H}^T \mathbb{H})$ (which is $c_1 - \beta_1$) via the quantum counting method outlined earlier yields the first Betti number.

As a brief summary, our algorithm mainly employs the matrix inversion and matrix multiplication technique to transform the initial 1-form $|w'\rangle$ to its harmonic representation. Quantum signal processing is then employed, combined with the quantum phase estimation plus repeating measurements to extract the Betti number. The main computational expenses come from matrix multiplication and inversion and the repetition of measurements required to estimate Betti numbers with sufficient accuracy. For the matrix multiplication/ inversion step, the matrices that appeared to have a dimension $c \times c$; therefore, these steps take $\mathcal{O}(\log(c))$ times (we ignore the sparsity dependent because it is very small, as we will see later). We emphasize a quite important point that, per Lemma 4, its running time also involves the conditional number, which can be large in general. This issue has been resolved in [24], where the authors provided a generalized quantum inversion method that allows a high conditional number matrix to be efficiently inverted. While the method in [24] induces a larger scaling on the sparsity, we note that the sparsity in our case is very small, as we will explicitly show in Appendix A. Therefore, we can safely integrate the result of [24] into our work without substantial further scaling. Further recall that $c = c_1 + c_2 \leq 2 \max(c_0, c_1, c_2)$, where $c_{0,1,2}$'s are the number of 0-simplices, 1-simplices and 2-simplices in the given complex, respectively. It is straightforward to see that $\mathcal{O}(\log(c)) = \mathcal{O}(\log(n))$ where n is the number of points. We state our main result in the following theorem.

Theorem 4 (Estimating 1st Betti number) *Let \sum be a simplicial complex with n points, corresponding to the triangulation of a 2-manifold. The 1st Betti number β_1 can be estimated to multiplicative accuracy δ_d in time*

$$\mathcal{O}\left(\frac{\log(n)}{\delta_d} \cdot \frac{c_r}{(c_r - \beta_r)}\right).$$

V. GENERALIZATION TO DIFFERENT BETTI NUMBERS AND HIGHER DIMENSIONAL MANIFOLDS

Given a triangulated 2-manifold, aside from the first, there are also the zeroth and the second Betti numbers β_0, β_2 . The zeroth Betti number is always one here, as we already assume that the given manifold is a connected graph that is triangulated. We have presented a quantum algorithm for the first Betti number. In order to compute β_2 , we first randomize a different 2-form Ω . We then deform them to the harmonic form by using the Hodge decomposition (2). The difference is that for a 2-manifold, there is no higher than 2-simplex; therefore, there will be no co-exact term. The decomposition is thus

$$\Omega = d\omega + h, \quad (32)$$

where ω is a 1-form, and h is the corresponding harmonic 2-form of Ω . We then follow the same procedure as we did for calculating β_1 .

The next important and somewhat subtle point is about higher dimensional cases. As we have emphasized from the beginning, the underlying groundwork of our method is the discrete Hodge theory. In order to apply this, for example, using Eqn. 2, we need to be able to formulate the operator $d\delta$ for all forms (see Eqn. 7). This formula depends on the dimension of the given manifold. The main reason is that, while the operator d is easily formulated in terms of a matrix given the simplex, the formulation of the operation δ relies on the Poincaré duality, which uses the concept of *dual cell*.

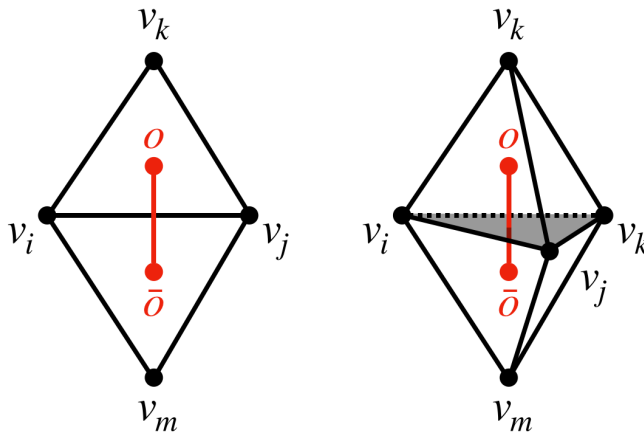


FIG. 2: Dual cell complexes in 2 and 3 dimensions. Left figure: In a triangulated 2-manifold, the dual to 2-simplex $[v_i, v_j, v_k]$ is a point o . The dual to an edge $[v_i, v_j]$ is an edge $o\bar{o}$. Right figure: In a triangulated 3-manifold, the dual to 3-simplex $[v_i, v_j, v_k, v_m]$ is a point o . The dual to a face (2-simplex) $[v_i, v_j, v_k]$ is an edge $o\bar{o}$.

For a triangulated 2-manifold, a dual cell to an edge (1-simplex) is an edge. However, for a triangulated 3-manifold, a dual cell to an edge is no longer an edge but a face (2-simplex). It means that even for the same first Betti number β_1 , the matrix coefficients (see Eqn. 7) are different. Fortunately, the computation procedure is the same, as it still relies on deforming a given k -form to its harmonic part. We can proceed with the computation of arbitrary Betti numbers and in arbitrary dimensional manifold in exactly the same way as we did in the above algorithm, provided the matrix form of δ (and hence $d\delta$) is given. Despite that there is no exact expression for δ , its matrix form can be efficiently calculated given the triangulation of the manifold (see Appendix B). Therefore, given a triangulated m -dimensional manifold Σ having n points, its r -th Betti number β_r can be estimated (with a multiplicative error δ_e) with time complexity

$$\mathcal{O}\left(\frac{\log(c_r)}{\delta_e} \cdot \frac{c_r}{(c_r - \beta_r)}\right),$$

where c_r is the number of r -simplices in Σ . In the low r limit ($r \ll n$), then $\log(c_r) \in \mathcal{O}(\log(n))$; whereas for the limit $r \sim n$, then $\log(c_r) \sim r \log(n)$. Our algorithm achieves its best performance when $\beta_r \ll c_r$, which is opposite to that of the LGZ [6, 13].

VI. FUERTHER ANALYSIS AND DISCUSSION

To make a comparison, we remind some of the results regarding the calculation of the first Betti number. As mentioned in [13], given a specified simplicial complex Σ with n points, the best classical algorithm to compute the first Betti number β_1 takes time $\mathcal{O}(c_1^3)$, where c_1 is the number of 1-simplices in Σ . As also mentioned in [13], the best running time of the improved-LGZ algorithm to estimate Betti number to multiplicative error δ is

$$\mathcal{O}\left(\frac{1}{\delta} n \kappa \sqrt{\frac{c_1}{\beta_1}}\right). \quad (33)$$

The advantage of the improved-LGZ algorithm compared to the classical algorithm is obtained in the regime $\beta_1 \rightarrow c_1$ (and generally, $\beta_k \rightarrow c_k$), as they emphasize in their work [13]. More specifically, in such a regime for a triangulated 2-manifold as in our specific case, the classical running time is $\mathcal{O}(n^3)$, since for a triangulation of n points, the number of edges (1-simplices) is bounded by $\mathcal{O}(n)$. The running time of the improved LGZ is (we ignore the κ factor) $\mathcal{O}(n/\delta)$. Hence, their quantum algorithm yields a cubic speedup.

In the same regime, our algorithm turns out to be slower than both above approaches, as c_1^2 will have the order $\sim \mathcal{O}(n^4)$. On the other hand, in the regime where β_1 is small compared to c_1 , our algorithm will have a running time

$$\mathcal{O}\left(\frac{\log(n)}{\delta}\right),$$

which is an exponential speedup compared to both the classical algorithm and that of the quantum algorithms (LGZ and its improved version) [6, 13]. Such an interesting opposite performance is a somewhat unexpected outcome from the duality between cohomology and homology.

Another subtle point that we would like to discuss is the assumption that we made regarding the shape of the simplicial complex. In our work, we only deal with a uniformly triangulated manifold, i.e., all the composing simplices are similar in size, and the manifold is built by properly gluing them together. In some previous works, such as [6, 9, 10, 13], the setting is seemingly more general where the shape can be arbitrary, as two points only get connected if their distance is smaller than a known threshold. One may wonder if our assumption would severely limit the practicality of the outlined algorithm. The answer is no, as the topology of the underlying manifold only depends on the connectivity but not the actual distance between arbitrary two points. As an example, let us consider the 2-dimensional case. One can imagine that, given a triangle with arbitrary angles/lengths, it is deformable or topologically equivalent to an equilateral triangle. Therefore, the topological space formed by the union, or by gluing different triangles together, is topologically equivalent to the union of equilateral triangles, which form the uniformly triangulated manifold. Since they are topologically equivalent, their underlying topological properties are the same. Consequently, performing computation on the uniformly triangulated manifold is more convenient, as we discuss further in Appendix B, where we provide an explicit formula for the codifferential operator. Finally, we remark that, in general, Hodge theory (see Theorem 2) works with closed manifolds (in both smooth and discrete settings). Therefore, the specification of a given simplicial complex requires an extra criterion. In the 2d case that we worked out earlier, each edge (1-simplex) is supposed to be adjacent to two triangles (2-simplex). The generalization to higher dimensions is straightforward. If our initial configuration is an open triangulated manifold, e.g., with a boundary, then a simple trick is to double cover the simplicial complex while preserving the symmetry. In this way, we can recover the closeness condition and proceed with our algorithm. As a final remark, while our framework requires more specification of the complex to ensure the close property, it requires exponentially fewer qubits and can potentially achieve exponentially faster running time. We regard it as a tradeoff factor.

VII. CONCLUSION

Our work has provided a ‘dual’ approach to [6] and is built upon the (discrete) Hodge theory and de Rham cohomology. There are a few major reasons underlying the advantage of our approach compared to [6]. In [6], the authors basically quantized the homology approach, associating the chain group to a vector space and finding singular values/ vectors of the boundary map ∂ . The key step in [6] is the identification of the chain group as a vector space, whereby each simplex is represented by a basis state, which means that the vector space needs to be at least as large as the number of simplices contained in Σ . By doing this way, the resource scales as a polynomial of n . In reality, the high value of n is usually desired (large-scale analysis), which means that $\text{poly}(n)$ could be very high, and hence the algorithm induces a very high computational cost. The cohomology approach we have adopted here fits nicely in such a large-scale setting. We recall that in (simplicial) cohomology, a cochain is a map $C \rightarrow R$ where C is some chain

group (space). Equivalently, we can imagine that each simplex is associated with a real number, and, therefore, we can have a more efficient way of storing our data, as we only need $\sim \log(M)$ qubits to store an M -dimensional vector, which further reduces the resource needed for processing. Another major point is that in [6], it is required to generate the proper simplicial complex state, which contributes substantially to the computational cost and, in certain cases, has a high failing probability (for details, see [6]). Here, in the cohomology approach, the initial 1-form state can, in fact, be chosen arbitrarily, which is more convenient. We further make an important remark that usually, the first and second Betti numbers are important enough for us to infer the underlying structure of a dataset, which implies that for those low Betti numbers, our algorithm actually has running time $\sim \mathcal{O}(\log(n))$. It is worth noting that our dual approach does not perform well in the regime of high Betti numbers, for which the LGZ algorithm works very well. Whether there is a mixed approach that can give rise to better performance in the intermediate regime is left for future exploration.

ACKNOWLEDGMENTS

This work was supported in part by the US Department of Energy, Office of Science, National Quantum Information Science Research Centers, Co-design Center for Quantum Advantage (C2QA) under contract number DE-SC0012704 (T.-C.W.), and by the National Science Foundation under Grants No. CMMI-1762287 (X.D.G.) and No. FAIN-2115095 (X.D.G.), as well as NIH 3R01LM012434-05S1 (X.D.G.) and NIH 1R21EB029733-01A1 (X.D.G.). We also acknowledge the support from a Seed Grant from Stony Brook University's Office of the Vice President for Research.

-
- [1] Larry Wasserman. Topological data analysis. *arXiv preprint arXiv:1609.08227*, 2016.
 - [2] Peter Bubenik et al. Statistical topological data analysis using persistence landscapes. *J. Mach. Learn. Res.*, 16(1):77–102, 2015.
 - [3] Xianfeng Gu, Yalin Wang, Tony F Chan, Paul M Thompson, and Shing-Tung Yau. Genus zero surface conformal mapping and its application to brain surface mapping. *IEEE Transaction on Medical Imaging (TMI)*, 23(8):949–958, 2004.
 - [4] Xianfeng David Gu and Shing-Tung Yau. *Computational conformal geometry*, volume 1. International Press Somerville, MA, 2008.
 - [5] Xianfeng Gu, Feng Luo, and Shing Tung Yau. Computational conformal geometry behind modern technologies. *Notices of the American Mathematical Society*, 67(10):1509–1525, 2020.
 - [6] Seth Lloyd, Silvano Garnerone, and Paolo Zanardi. Quantum algorithms for topological and geometric analysis of data. *Nature communications*, 7(1):1–7, 2016.
 - [7] A Yu Kitaev. Quantum measurements and the abelian stabilizer problem. *arXiv preprint quant-ph/9511026*, 1995.
 - [8] Dominic W Berry, Graeme Ahokas, Richard Cleve, and Barry C Sanders. Efficient quantum algorithms for simulating sparse hamiltonians. *Communications in Mathematical Physics*, 270(2):359–371, 2007.
 - [9] Shashanka Ubaru, Ismail Yunus Akhalwaya, Mark S Squillante, Kenneth L Clarkson, and Lior Horesh. Quantum topological data analysis with linear depth and exponential speedup. *arXiv preprint arXiv:2108.02811*, 2021.
 - [10] Sam McArdle, András Gilyén, and Mario Berta. A streamlined quantum algorithm for topological data analysis with exponentially fewer qubits. *arXiv preprint arXiv:2209.12887*, 2022.
 - [11] Sam Gunn and Niels Kornerup. Review of a quantum algorithm for betti numbers. *arXiv preprint arXiv:1906.07673*, 2019.
 - [12] Bernardo Ameneyro, Vasileios Maroulas, and George Siopsis. Quantum persistent homology. *arXiv preprint arXiv:2202.12965*, 2022.
 - [13] Alexander Schmidhuber and Seth Lloyd. Complexity-theoretic limitations on quantum algorithms for topological data analysis. *arXiv preprint arXiv:2209.14286*, 2022.
 - [14] Aram W Harrow, Avinandan Hassidim, and Seth Lloyd. Quantum algorithm for linear systems of equations. *Physical review letters*, 103(15):150502, 2009.
 - [15] Seth Lloyd, Masoud Mohseni, and Patrick Rebentrost. Quantum principal component analysis. *Nature Physics*, 10(9):631–633, 2014.
 - [16] Andrew M Childs, Robin Kothari, and Rolando D Somma. Quantum algorithm for systems of linear equations with exponentially improved dependence on precision. *SIAM Journal on Computing*, 46(6):1920–1950, 2017.
 - [17] Nhat A Nghiem and Tzu-Chieh Wei. An improved method for quantum matrix multiplication. *Quantum Information Processing*, 22(8):299, 2023.
 - [18] Guang Hao Low and Isaac L Chuang. Optimal hamiltonian simulation by quantum signal processing. *Physical review letters*, 118(1):010501, 2017.
 - [19] Guang Hao Low and Isaac L Chuang. Hamiltonian simulation by qubitization. *Quantum*, 3:163, 2019.
 - [20] András Gilyén, Yuan Su, Guang Hao Low, and Nathan Wiebe. Quantum singular value transformation and beyond: exponential improvements for quantum matrix arithmetics. In *Proceedings of the 51st Annual ACM SIGACT Symposium*

on *Theory of Computing*, pages 193–204, 2019.

- [21] Raoul Bott, Loring W Tu, et al. *Differential forms in algebraic topology*, volume 82. Springer, 1982.
- [22] Nathan Wiebe, Daniel Braun, and Seth Lloyd. Quantum algorithm for data fitting. *Physical review letters*, 109(5):050505, 2012.
- [23] Gilles Brassard, Peter Hoyer, Michele Mosca, and Alain Tapp. Quantum amplitude amplification and estimation. *Contemporary Mathematics*, 305:53–74, 2002.
- [24] B David Clader, Bryan C Jacobs, and Chad R Sprouse. Preconditioned quantum linear system algorithm. *Physical review letters*, 110(25):250504, 2013.
- [25] Mikio Nakahara. *Geometry, topology and physics*. CRC press, 2018.

Appendix A: Further elaboration on linear equation

Some necessary background on topology and geometry can be found in any standard textbook, such as [25]. In this section, we discuss in detail how to solve for Ω and η that appear in the Hodge decomposition (3), which constitutes the linear equation similar to Eq. (7) that we will solve with a quantum means. The Hodge decomposition holds for arbitrary dimensions, but since we deal with a triangulated 2-manifold and present how to compute the first Betti number β_1 , we proceed in this section with the case of 1-forms. Further generalization to higher dimensions will be left for the next section, which allows for the adoption by our quantum procedure.

Let ω be some 1-form. Recall that the Hodge decomposition allows ω to be written as

$$\omega = \delta\Omega + d\eta + h, \quad (\text{A1})$$

where Ω is a 2-form, η is a 0-form and h is called the harmonic form, d is the exterior derivative, which maps from the space of 0-form to 1-form, and δ is the codifferential operator, which maps a 2-form to a 1-form. We note that h vanishes under d and δ : $dh = 0$ and $\delta h = 0$. These two operators have a special property:

$$d^2 \equiv d \circ d = 0,$$

and

$$\delta^2 \equiv \delta \circ \delta = 0.$$

Applying the derivative map d to both sides of Eqn. A1, and using the above properties of both the derivative map and the harmonic form, we obtain:

$$d\omega = d\delta\Omega. \quad (\text{A2})$$

We have mentioned that in the discrete context, an arbitrary k -form is approximated by a k -cochain. Let $[v_1, v_2, v_3]$ be a 2-simplex, then we have:

$$d\omega[v_1, v_2, v_3] = d\delta\Omega[v_1, v_2, v_3]. \quad (\text{A3})$$

From the above equation, we have

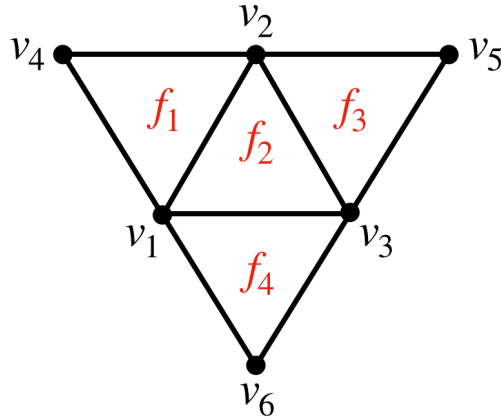


FIG. 3: A part of triangulated 2-manifold. Each face (2-simplex) is labeled with red color.

$$d\omega[v_1, v_2, v_3] = \omega[v_1, v_2] + \omega[v_2, v_3] + \omega[v_3, v_1].$$

If ω is known, then we can compute $d\omega[v_1, v_2, v_3]$. Likewise:

$$d\delta\Omega[v_1, v_2, v_3] = \delta\Omega[v_1, v_2] + \delta\Omega[v_2, v_3] + \delta\Omega[v_3, v_1].$$

A standard procedure using the Poincaré duality to formulate δ is done in the standard textbook, such as [4]. Here we quote the results. From Fig. 3, f_1 and f_2 are two faces (2-simplices) adjacent to $[v_1, v_2]$. We then have the following formula for $\delta\Omega[v_1, v_2]$:

$$\delta\Omega[v_1, v_2] = \frac{1}{w_{12}} \left(\frac{\Omega(f_1)}{|f_1|} - \frac{\Omega(f_2)}{|f_2|} \right), \quad (\text{A4})$$

where $|f_{1,2}|$ is the area of the corresponding faces, or 2-simplices, and w_{12} is the cotangent edge weight (see in Fig. 3 for the illustration),

$$w_{12} = \frac{1}{2} \left(\cot(\angle v_1 v_3 v_2) + \cot(\angle v_1 v_4 v_2) \right).$$

The above formula for the cotangent edge weight needs to be slightly modified if the edge $[v_1, v_2]$ lies on the boundary (for example, edge $[v_1, v_4]$ on Fig. 3), which means that there is only one face adjacent to it. In such a case, then we only include the cotangent of one angle, which is opposite to $[v_1, v_4]$ ($\angle v_1 v_2 v_4$).

Applying formula A4, we then obtain a full formula for $d\delta\Omega[v_1, v_2, v_3]$, which is:

$$d\delta\Omega[v_1, v_2, v_3] = \frac{1}{w_{12}} \left(\frac{\Omega(f_1)}{|f_1|} - \frac{\Omega(f_2)}{|f_2|} \right) + \frac{1}{w_{23}} \left(\frac{\Omega(f_3)}{|f_3|} - \frac{\Omega(f_2)}{|f_2|} \right) + \frac{1}{w_{13}} \left(\frac{\Omega(f_4)}{|f_4|} - \frac{\Omega(f_2)}{|f_2|} \right). \quad (\text{A5})$$

We recall that $d\omega[v_1, v_2, v_3] = d\delta\Omega[v_1, v_2, v_3]$, and as ω is known, we obtain an algebraic equation for Ω . We note that the Eqn. A5 contains the first order of Ω (acting on certain 2-simplices), and, therefore, repeating equation A3 eventually yields a linear equation (Eqn. 7), and the solution is unique [4]. We note that, the coefficients of matrix A in Eqn. 7 in general will include terms of the following form

$$\frac{1}{w \cdot |f|},$$

where w is a cotangent edge weight, and $|f|$ is the area of some 2-simplex. In general, these quantities can be computed provided the pairwise distance between vertices that form the corresponding simplices. In our problem, we are working with a *uniform* triangulated manifold, which means that all the 2-simplices or triangles are equilateral. Therefore, the cotangent edge weight is simply:

$$w = \frac{1}{2} \left(\frac{1}{\sqrt{3}} + \frac{1}{\sqrt{3}} \right) = \frac{1}{\sqrt{3}}$$

for all cotangent edge weights (including the internal ones) and the value of $|f|$ is

$$|f| = \frac{\sqrt{3}a^2}{2},$$

where a is the distance between arbitrary two connected points, or 0-simplices. The value a depends on the given dataset and, in principle, it can be arbitrary, as the length does not affect the topology of a given configuration.

Now, we elaborate on the computation of the 0-form η in Eqn. A1. By applying δ to both sides of Eqn. A1, we have:

$$\delta\omega = \delta d\eta.$$

As $\delta\omega$ is a 0-form, using the same method of the Poincaré duality [4], the formula for $\delta\omega$ acting on some 0-simplex or a point v_0 is:

$$\delta\omega[v_0] = -\frac{1}{|\tilde{v}_0|} \sum_{v_i \sim v_0} w_{0j} \cdot \omega[v_0, v_j], \quad (\text{A6})$$

where the symbol \sim denotes the adjacency (i.e., vertex v_j is connected to v_0 via an edge), w_{0j} is the cotangent edge weight (defined above), and $|\tilde{v}_0|$ is the area of the dual cell complex of v_0 (we will elaborate further the dual cell complex in the subsequent section).

The formulation of $\delta d\eta$ is the same, as $d\eta$ is also a 1-form. More explicitly, we have:

$$\delta d\eta[v_0] = -\frac{1}{|\tilde{v}_0|} \sum_{v_i \sim v_0} w_{0j} \cdot d\eta[v_0, v_j] = -\frac{1}{|\tilde{v}_0|} \sum_{v_i \sim v_0} w_{0j} \cdot (\eta[v_j] - \eta[v_0]).$$

Since $\delta\omega = \delta d\eta$, the area term $|\tilde{v}_0|$ cancels out, fortunately. By applying the above formulas for all vertices, eventually, we obtain a linear equation for η with known coefficients w 's, i.e., from the cotangent edge weights.

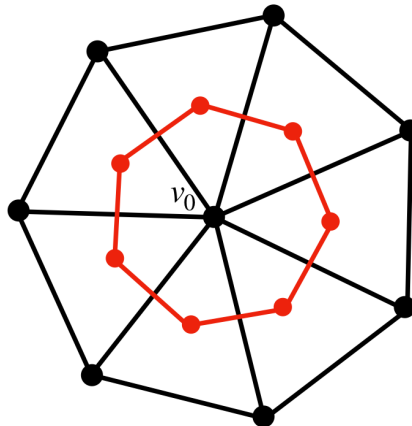


FIG. 4: Illustration of dual cell of 0-simplex v_0 . The whole region inside the red-colored boundaries is the dual cell of v_0 , with area denoted as $|\tilde{v}_0|$. This area could be computed given the pairwise distance between v_0 and its adjacent vertices. In our case where the given triangulation is uniform and the distance between two vertices is a , it is easy to calculate the area $|\tilde{v}_0|$, which is $pa^2/4\sqrt{3}$, where p is the number of adjacent points to v_0 .

Appendix B: General Version of Discrete Hodge Theory

As we have emphasized, going to higher dimensional manifolds incurs more complication, as the rule for $d\delta$ and δd that we described in the previous section will no longer hold exactly in the same form. The main reason is due to the use of the Poincaré duality. The dual cell to each simplex is generally different for different dimensions. Hence, it affects how we formulate the codifferential operator δ (and its composition with d). We remark that the underlying theory of our algorithm relies on results from non-trivial geometry and topology, which means that we do not expect to cover everything here, and we refer the readers to the literature, such as [25], and particularly, more relevant to our perspective from computational algorithms, Ref. [4]. In this section, we aim to exemplify the subtle points regarding the generalization of our algorithm to higher dimensions in more detail than what we have described in Sec. V.

1. Poincare Dual Cell Complex

We first review the concept of the Poincaré dual cell complex. The key point is that, given a triangulated manifold of some dimension n , the dual cell of some k -simplex is not necessarily a proper simplex.

As we can see from Fig. 5, the order of the given simplex (e.g., 0, 1, or 2-simplex) and of its dual cell match the dimension of a given manifold, which is 2. In the 2d case, the dual cell to a 2-simplex, denoted by f (rightmost ones), is a point \bar{f} (of zero order), which is the center of the circle that passes all three points of the original 2-simplex f . In the middle two figures, the 1-simplex e has the dual cell \bar{e} . The way \bar{e} is constructed is as follows. First, we construct the dual cell of the two triangles, or 2-simplices, that are adjacent to e , which are two points. Then we connect them, hence forming a line \bar{e} . Likewise, for the leftmost figures, the dual cell of a given point or 0-simplex v is formed by connecting the dual cells of all triangles (2-simplex) that v belongs to, including the interior. Hence, according to the bottom left figure, the dual cell of v , \bar{v} is the region inside the red lines, including the boundary. A similar construction holds for a triangulated manifold of arbitrary dimension.

2. Codifferential Operator

Let M be a triangulated n -dimensional manifold. Now, we examine the codifferential operator $\delta : \Omega^k \rightarrow \Omega^{k-1}$, where Ω^k is the space of k -form ($k < n$). Let σ be some $(k-1)$ simplex and $\bar{\sigma}$ be its corresponding Poincaré dual-cell complex. Additionally, let $\partial\bar{\sigma} = \sum_i \gamma_i$ be the boundary of $\bar{\sigma}$, where in general, γ_i is some simplex (the orientation is included). Let Δ be some k -form. We recall that, as we have mentioned in the main text, in the discrete setting, a

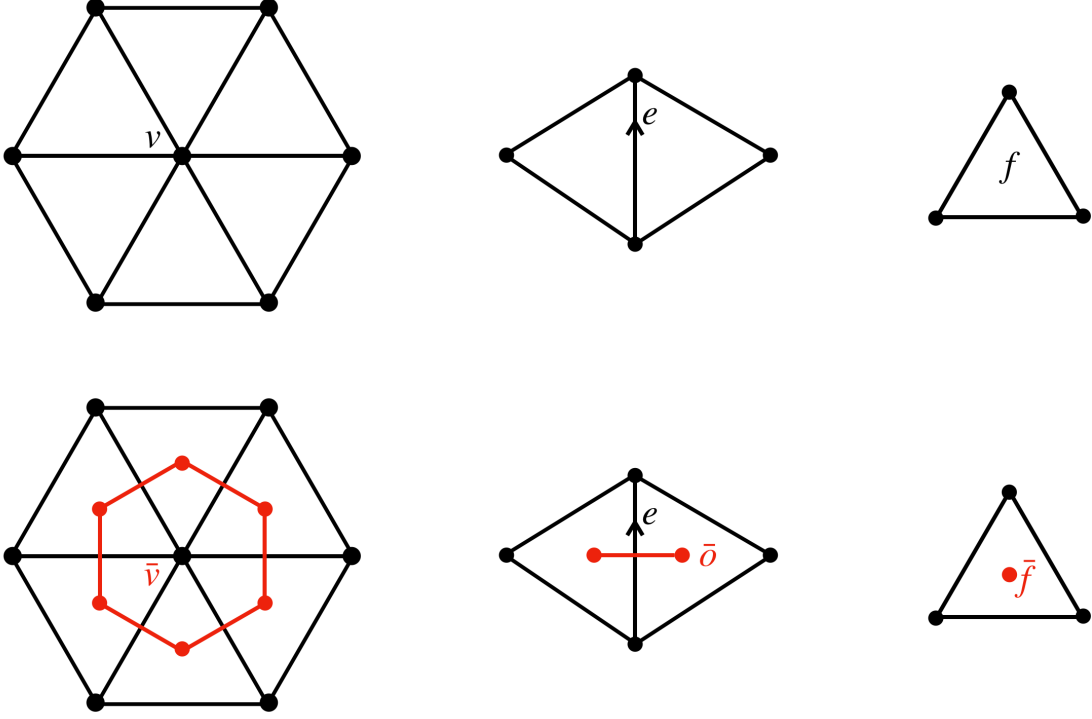


FIG. 5: Dual cell complex in 2-d case

form is identical to a *cochain*. We have thus the following general formula:

$$\delta\Delta(\sigma) = (-1)^{nk+n+1}(-1)^{(n-k+1)(k-1)} \frac{|\sigma|}{|\bar{\sigma}|} \sum_i \frac{|\gamma_i|}{|\bar{\gamma}_i|} \Delta(\bar{\gamma}_i). \quad (\text{B1})$$

The above formula is somewhat complicated, but it is straightforward since, in the previous section, we have provided a systematic way to construct a dual-cell complex. Given an n -dim triangulated manifold, we can, in principle, construct the corresponding dual-cell complex and can then carry out the formula for δ algorithmically. Given distances between points on the original manifold M , in principle, we can compute the corresponding length, area, and volume for elements of simplices of M , as well as for their dual cell complex. In the case of uniform triangulation, the calculation is much easier, as we have computed some quantities like w and $|f|$ in the previous section. Therefore, all the linear systems (such as in Eqn. (7)) are entry-wise accessible.

We will exemplify the formula B1 further for both 2-dim and 3-dim cases by direct calculation. In the previous section A, we already encounter the formulation. We will try to reproduce the same formulas for $\delta\Omega$ and δw in 2d case.

2-dimensional Triangulated Manifold

Let Ω be 2-form (or 2-cochain) and ω be 1-form (or 1-cochain). First, we try to apply (B1) to compute $\delta\Omega(e)$ on the right of Fig. 6. According to the figure, the dual cell of the triangle $f_1 = [v_0, v_1, v_2]$ is denoted as \bar{o} , and the dual cell of triangles $f_2 = [v_0, v_1, v_3]$ is o . The dual cell of e , or 1-simplex $[v_0, v_1]$, is $\bar{e} = o\bar{o}$. Applying Eqn. B1, we have

$$\delta\Omega(e) = \frac{|e|}{|\bar{e}|} \left(\frac{|o|}{|\bar{o}|} \Omega(\bar{o}) - \frac{|\bar{o}|}{|o|} \Omega(o) \right).$$

Since both o and \bar{o} are points, $|o|$ and $|\bar{o}|$ are equal to 1. Furthermore, the dual of o and \bar{o} are $[v_0, v_1, v_3]$, $[v_0, v_1, v_2] \equiv f_1, f_2$, respectively, as we defined in the previous section. A result from elementary geometry [4] shows that

$$\frac{|\bar{e}|}{|e|} = \frac{1}{2} (\cot(\angle v_1 v_3 v_0) + \cot(\angle v_1 v_2 v_0)) = w_{12},$$

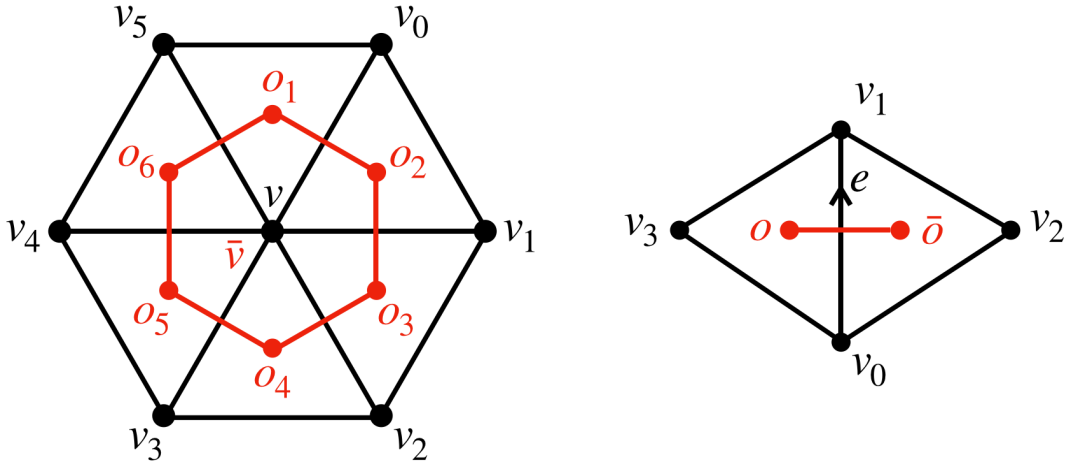


FIG. 6: Dual cell complex of a vertex and an edge.

which is defined as the cotangent edge weight. Combining everything, we obtain:

$$\delta\Omega(e) = \frac{1}{w_{12}} \left(\frac{1}{f_1} \Omega(f_1) - \frac{1}{f_2} \Omega(f_2) \right), \quad (\text{B2})$$

which is exactly what we got in Eqn. A4. A similar calculation can be done for $\delta\omega$, which leads to a similar form as in Eqn. A6.

3-dimensional Triangulated Manifold

In the 3d case, the situation is a bit more complicated because the dual of each simplex is no longer the same as in the 2d case. However, the formulation is still straightforward, as we can systematically construct the dual cell and use the same formula B1. We work out the following example; see figure 7.

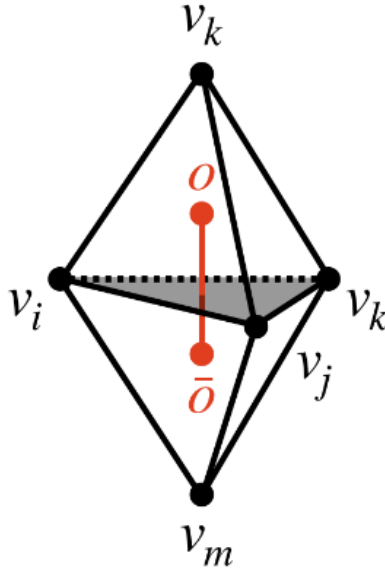


FIG. 7: Example in 3-D

We denote the 2-simplex $\sigma = [v_i, v_j, v_k]$ and its dual cell $\bar{\sigma} = o\bar{o}$; we further denote 3-simplex $[v_n, v_i, v_j, v_k], [v_m, v_i, v_j, v_k]$ as α, β . Let Ω be some 3-form. The boundary of $\bar{\sigma}$ is:

$$\partial\bar{\sigma} = \bar{o} - o$$

The action of $\delta\Omega(\sigma)$ is:

$$\delta\Omega(\sigma) = \frac{|\sigma|}{|o\bar{o}|} \left(\frac{1}{|\alpha|} \Omega(\alpha) - \frac{1}{|\beta|} \Omega(\beta) \right). \quad (\text{B3})$$

Since the 3-simplex is a tetrahedron, its volume is $V = |\alpha| = |\beta| = a^3/6\sqrt{2}$, and the length of $o\bar{o}$ is $a/\sqrt{6}$; the area of σ is $|\sigma| = \sqrt{3}a^2/4$.

Appendix C: Product of Block Encoding

Here we explicitly show that, given a unitary block encoding for matrices A_1 and A_2 , respectively, one can construct the unitary block encoding of A_1A_2 , or A_2A_1 with a few modest steps. While it has been established in the original work [20], we present a solution here for completeness.

Let U_1, U_2 be block encoding of A_1, A_2 , i.e, we have:

$$U_{1,2} = \begin{pmatrix} A_{1,2} & \cdot \\ \cdot & \cdot \end{pmatrix}.$$

Equivalently, we can write U (we drop the subscript for now, as it should not cause any confusion):

$$U = |\mathbf{0}\rangle \langle \mathbf{0}| \otimes A + \dots$$

We now observe the following property:

$$U |\mathbf{0}\rangle |\phi\rangle = |\mathbf{0}\rangle A |\phi\rangle + \sum_{j \neq \mathbf{0}} |j\rangle |\phi_j\rangle, \quad (\text{C1})$$

where $|\phi\rangle$ and all $|\phi_j\rangle$ (the latter being essentially garbage states) have the same dimension as matrix A . For a reason that will be clear later on, we borrow an extra qubit initialized in $|0\rangle$ and rewrite the above equation as:

$$\mathbb{I} \otimes U |\mathbf{0}\rangle |\phi\rangle = |0\rangle |\mathbf{0}\rangle A |\phi\rangle + |0\rangle \sum_{j \neq \mathbf{0}} |j\rangle |\phi_j\rangle. \quad (\text{C2})$$

Now we use X gate to flip the ancilla qubit to obtain the state:

$$|1\rangle |\mathbf{0}\rangle A |\phi\rangle + |1\rangle \sum_{j \neq \mathbf{0}} |j\rangle |\phi_j\rangle.$$

Denote the whole above unitary process, which maps $|0\rangle |\mathbf{0}\rangle |\phi\rangle$ to $|1\rangle |\mathbf{0}\rangle A |\phi\rangle + |1\rangle \sum_{j \neq \mathbf{0}} |j\rangle |\phi_j\rangle$ as \mathcal{U} . For matrix A_1 , given a computational basis state $|i\rangle$, we have:

$$\mathcal{U}_1 |0\rangle |\mathbf{0}\rangle |i\rangle = |1\rangle |\mathbf{0}\rangle A_1 |i\rangle + |1\rangle \sum_{j \neq \mathbf{0}} |j\rangle |\phi_j\rangle. \quad (\text{C3})$$

For matrix A_2 , we would use the conjugate transpose of the original U_2 (without the extra CNOT step that flips the ancilla) to obtain:

$$U_2^\dagger |0\rangle |\mathbf{0}\rangle |k\rangle = |0\rangle |\mathbf{0}\rangle A_2^\dagger |k\rangle + |0\rangle \sum_{j \neq \mathbf{0}} |j\rangle |\phi_j\rangle. \quad (\text{C4})$$

Now for the above state, we use the second register (associated with $|\mathbf{0}\rangle$) as controlling qubits to flip the first qubit $|0\rangle$ to $|1\rangle$, conditioned on it being $|\mathbf{0}\rangle$. In other words, from the above state, we obtain:

$$|1\rangle |\mathbf{0}\rangle A_2^\dagger |k\rangle + |0\rangle \sum_{j \neq \mathbf{0}} |j\rangle |\phi_j\rangle. \quad (\text{C5})$$

We denote the process containing of U_2 and the controlled-X step above as \mathcal{U}_2 , i.e.,

$$\mathcal{U}_2 |0\rangle |\mathbf{0}\rangle |k\rangle = |1\rangle |\mathbf{0}\rangle A_2^\dagger |k\rangle + |0\rangle \sum_{j \neq \mathbf{0}} |j\rangle |\phi_j\rangle. \quad (\text{C6})$$

It is straightforward to observe that, thanks to the orthogonality of computational basis states, the inner product:

$$\langle 0 | \langle \mathbf{0} | \langle k | \mathcal{U}_2^\dagger \mathcal{U}_1 | 0 \rangle | \mathbf{0}, i \rangle = \langle k | A_2 A_1 | i \rangle \equiv (A_2 A_1)_{ki}, \quad (\text{C7})$$

which is exactly the definition of unitary block encoding. Therefore, we have successfully constructed the block encoding of $A_2 A_1$. For the reverse order $A_1 A_2$, the procedure is exactly the same, as we just need to reverse the role of $\mathcal{U}_{1,2}$ from the above procedure.